scientific reports

Check for updates

OPEN

Evaluation of dECM hydrogel-NAP on 3D organotypic human corneal epithelium in diabetic keratopathy model

Simona Casarella[1], Nicoletta Palmeri[2], Agata Grazia D'Amico[3], Assunta Virtuoso[4], Salvatore Saccone[5], Elisabetta Pricoco[6], Davide Scollo[7], Antonio Longo[8], Michele Papa[4], Francesca Boccafoschi[1], Velia D'Agata[2] & Grazia Maugeri[2]✉

Diabetes mellitus, a global epidemic, is a leading cause of blindness due to its detrimental effects on the retina, lens, and cornea. Diabetic keratopathy (DK), a significant ocular complication, severely compromises the corneal epithelium structure, barrier function, and healing capacity, largely driven by hyperglycemia-induced oxidative stress and apoptosis. Current therapeutic strategies for DK are limited and primarily symptomatic, failing to address underlying cellular deficits. This study investigates a novel regenerative approach utilizing a decellularized extracellular matrix (dECM) hydrogel functionalized with the neuroprotective peptide NAP (dECM hydrogel-NAP). Both dECM hydrogels and NAP have demonstrated promising regenerative and protective properties in various tissues, though their combined efficacy for diabetic corneal repair remains unexplored. Using a three-dimensional (3D) organotypic human corneal epithelium model of DK, we evaluated the therapeutic potential of dECM hydrogel-NAP to promote epithelial wound healing, restore barrier function, mitigate apoptotic responses, and support cellular viability under diabetic conditions. Our findings suggest that dECM hydrogel-NAP holds significant promise as a therapeutic strategy for supporting corneal epithelial regeneration in diabetic keratopathy.

Keywords Diabetic keratopathy, DECM hydrogel, NAP, 3D organotypic culture

Diabetes mellitus, the fastest growing global public health concern[1], is a well-established cause of ocular issues and represents one of the major contributors to blindness in developed nations, due to its deleterious effects on the retina, lens and cornea[2,3].

The corneal epithelium plays a crucial role in preventing eye infections and maintaining the cornea's clarity and stability. Timely repair of epithelial damage is essential for restoring vision. However, diabetic keratopathy (DK) affects the corneal epithelium by altering its structure and increasing its fragility, disrupting the basement membrane, impairing epithelial attachment and healing, and compromising its barrier function[4]. Furthermore, diabetes can cause corneal nerve damage and changes in the corneal stroma, Descemet's membrane, and endothelium[5,6]. The complex pathophysiology of DK involves hyperglycemia-induced oxidative stress and inflammation, leading to apoptosis. The increased rates of programmed cell death are observed in different corneal cell types, particularly in epithelial cells[7]. Elevated apoptosis in epithelial cells compromises the integrity of the corneal barrier, affecting proper wound closure[8].

[1]Department of Health Sciences, Università del Piemonte Orientale, Novara 28100, Italy. [2]Section of Anatomy, Histology and Movement Sciences, Department of Biomedical and Biotechnological Sciences, University of Catania, Catania 95123, Italy. [3]Department of Drug Sciences, University of Catania, Catania, Italy. [4]Division of Human Anatomy, Neuronal Morphology Networks & Systems Biology Lab, Department of Mental and Physical Health and Preventive Medicine, University of Campania Luigi Vanvitelli, Naples 80138, Italy. [5]Department of Biological, Geological and Environmental Sciences, Section of Animal Biology, University of Catania, Catania 95123, Italy. [6]Anatomic Pathology, A.O.U. Policlinico G. Rodolico-San Marco, Catania, Italy. [7]Eye Clinic Catania University San Marco Hospital, Viale Carlo Azeglio Ciampi, Catania 95121, Italy. [8]Department of Ophthalmology, University of Catania, Catania 95123, Italy. ✉email: graziamaugeri@unict.it

Despite scientific community efforts, effective therapeutic strategies for DK remain limited and primarily focused on symptomatic relief rather than addressing the underlying cellular and molecular deficits. In this scenario, decellularized extracellular matrix (dECM) hydrogels have emerged as highly promising biomaterials in regenerative medicine[9]. Derived from native tissues, dECM hydrogels retain the complex biochemical cues and structural components of the original extracellular matrix (ECM), providing a biocompatible and bioactive scaffold that can promote cell adhesion, proliferation, differentiation, wound healing and tissue remodeling[9–11]. Recently, bovine pericardium dECM hydrogel has demonstrated to be biocompatible in vitro and in vivo, facilitating wound closure and demonstrating its great potential for regenerative applications[10,12]. Nevertheless, the ability of this hydrogel to repair damaged diabetic cornea has not been investigated. Concurrently, a small peptide derived from activity-dependent neuroprotective protein (ADNP), known as NAP, have demonstrated significant antioxidant, anti-apoptotic and protective properties in tissues and cells of various organs[13–15]. In the eye, studies showed that intravitreal administration of NAP protects rat retinal ganglion cells (RGCs) after retinal ischemia and optic nerve crush[16]. NAP treatment provided corneal protection against ultraviolet B (UV-B) radiations induced apoptosis[17,18]. Moreover, NAP prevented hyperglycemia/hypoxia-induced apoptosis in vivo and in vitro model of diabetic retinopathy[19–22]. Hence, this study aims to evaluate the therapeutic efficacy of a novel dECM hydrogel functionalized with NAP (dECM hydrogel-NAP) on a three-dimensional (3D) organotypic human corneal epithelium model of DK. By utilizing a 3D model that closely mimics the human corneal epithelium, we seek to investigate the capacity of dECM hydrogel-NAP to promote epithelial wound healing, restore barrier function, mitigate apoptotic responses, and support cellular viability under diabetic conditions. Results suggest the potential of dECM hydrogel-NAP as a therapeutic approach for supporting corneal epithelial regeneration under DK.

Results

Optical properties of dECM hydrogel

The cornea is a transparent tissue refracting most of the light entering the eye to the lens and retina, the hydrogel suitable for the cornea tissue must have similar light transmittance properties. The hydrogel provided by Tissuegraft was extensively characterized for the use with regenerative purposes as reported previous studies[12,10]. In order to select the optimal concentration for corneal use, we characterized the visible light (595 nm) transmittance of dECM hydrogel at different concentrations (9 mg/ml, 4 mg/ml and 2 mg/ml) (Fig. 1). In Fig. 1b, the transmittance in the visible light range is shown over time. After 1 week the 2 mg/ml maintained the transmittance slightly decreased from 92% to around 89%, which is similar to that of the human cornea (87%)[23,24]. Moreover, the transmittance remained the same over one week, suggesting to consider this concentration as carrier matrix for NAP enrichment. After two weeks the transmittance of the hydrogel was decreased in all the concentrations.

Then, we evaluated the light transmission in presence of the peptide (Fig. 1c). The dECM 2 mg/ml with NAP smoothly decreased the transmittance of the hydrogel compared to dECM 2 mg/ml alone but did not

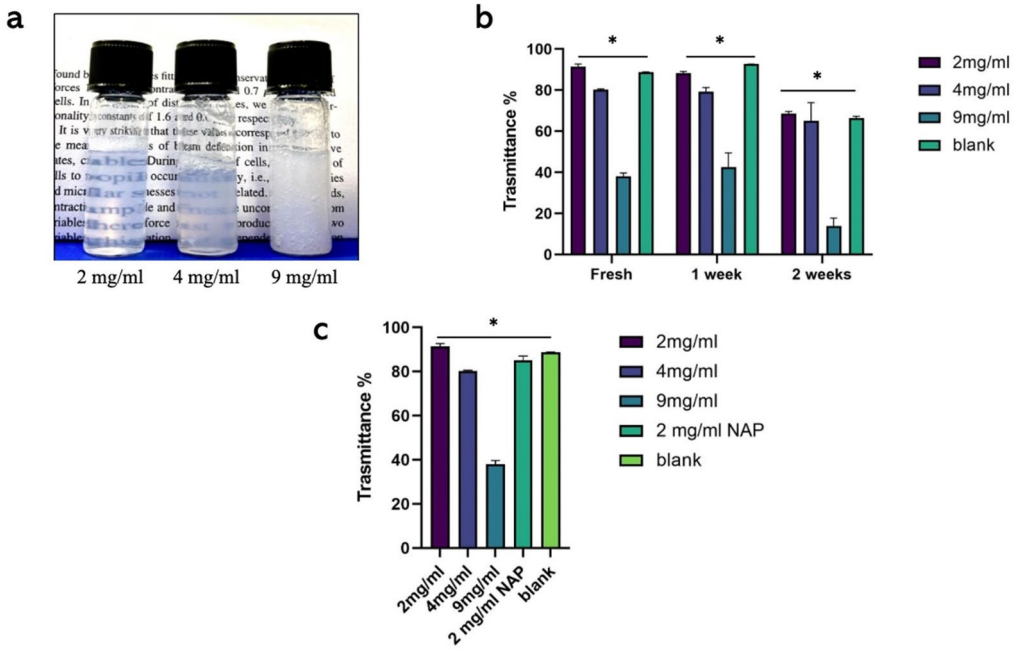

Fig. 1. Transmittance of dECM hydrogels over time. (**a**) General transparency observation of hydrogels at different concentrations. (**b**) Light transmission of hydrogels at visible light. Results represented from three different experiments. The bar graphs show quantitative analysis obtained by three independent experiments. Data represent means ± SD. *p-value ≤ 0.05.

alter the overall optical properties, remaining around the 85% of average transmittance, confirming the optimal concentration for the corneal application.

Biocompatibility of dECM hydrogel

Biocompatibility of the dECM hydrogel is critical to support corneal epithelium regeneration. To establish its biocompatibility and determine the optimal concentration for subsequent experiments, we performed, MTT assay was performed in human corneal epithelial cells (hCECs) and Statens Seruminstitut rabbit corneal (SIRC) epithelial cells at 24 and 72 h, by using 9 mg/mL or 6 mg/mL or 4 mg/mL, or 2 mg/mL of dECM hydrogel. As shown in Fig. 2, hCECs seeded with 9 mg/mL dECM hydrogel showed a significant reduction in cell number as compared to the control (**$p < 0.01$). At 72 h, both hCECs (Fig. 2a) and SIRC cells (Supplementary Fig. 1a) seeded with 9 mg/mL or 6 mg/mL, or 4 mg/mL dECM hydrogel significantly reduced their cell number (***$p < 0.001$ and ****$p < 0.0001$).

The cytotoxic potential of the biomaterials on dECM hydrogel was evaluated by spectrophotometric quantification of the LDH released in culture medium. The extracellular LDH activity in hCECs seeded with 9 mg/mL or 6 mg/mL dECM hydrogel was increased at 24 h and 72 h, as compared to the control group (***$p < 0.001$ and ****$p < 0.0001$) (Fig. 2b). At 72 h, also SIRC cells cultured with 9 mg/mL or 6 mg/mL dECM hydrogel showed a significant increased cytotoxicity as compared to control (****$p < 0.0001$) (Supplementary Fig. 1b). These results indicated that the optimal concentration of dECM hydrogel in terms of cytocompatibility is 2 mg/ml, which was the concentration used in all subsequent experiments with NAP, whose concentration (10 nM) was chosen based on efficacy in previous works[17,18,20,21].

Next, we investigated the effect of NAP alone or in combination with the 2 mg/mL dECM hydrogel on cell viability. As shown in Supplementary Fig. 1c, at 72 h, SIRC cells treated with NAP showed an increase in cell number as compared to control (*$p < 0.05$). Both hCECs and SIRC cells cultured with dECM hydrogel + NAP showed a significant increase in cell number (Fig. 2c and Supplementary Fig. 2c). Moreover, Phalloidin staining (Fig. 3) performed at 3 and 7 days, reveals how the presence of the dECM hydrogel with or without the presence of NAP did not alter the morphological properties of the primary human corneal epithelial cells (PCs) cells.

Effect of dECM hydrogel-NAP on corneal epithelium healing

We performed a wound healing assay to evaluate the effect of the dECM hydrogel-NAP on the migration of corneal epithelial cells and wound repair capability. As shown in Fig. 4, at 24 h after confluent hCECs were scratched, a significant wound closure was observed when cells were seeded with NAP and even more in the

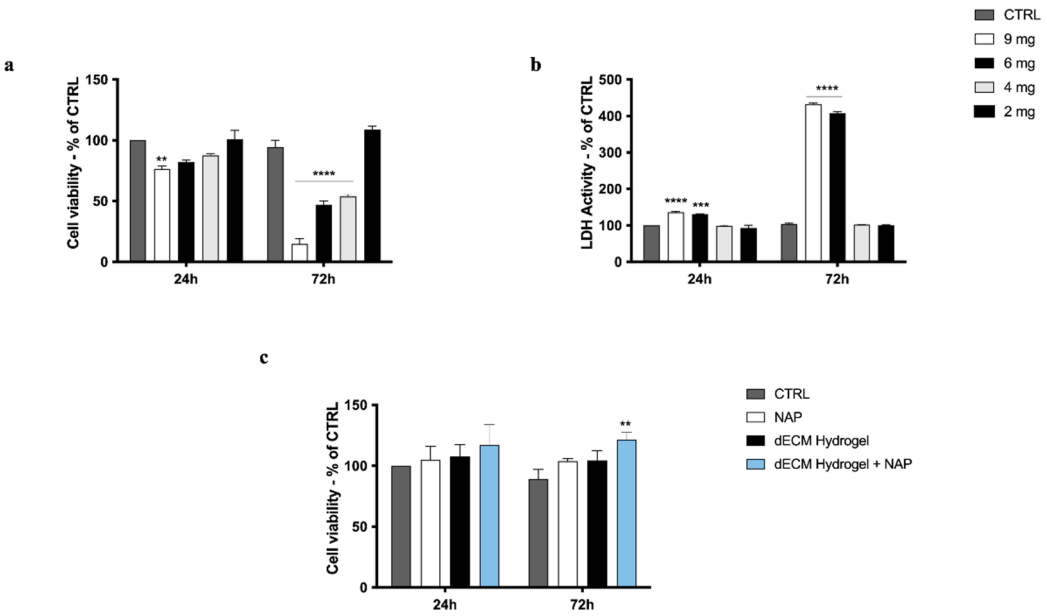

Fig. 2. Cytocompatibility of dECM hydrogel. (**a**) The relative percentage increase or decrease in hCECs number was measured at 24 h and 72 h in cells cultured in different dECM hydrogel concentrations. The bar graphs show quantitative analysis obtained by three independent experiments. Data represent means ± SEM. **$p < 0.01$ vs. CTRL 24 h; ****$p < 0.0001$ vs. CTRL 72 h by one-way ANOVA. (**b**) Extracellular LDH activity in hCECs cultured in different hydrogel concentrations for 24–72 h. The extracellular LDH activity was measured using CyQUANT™ LDH cytotoxicity assay kit according to the manufacturer's instructions. The bar graphs show quantitative analysis obtained by three independent experiments. ***$p < 0.001$; ****$p < 0.0001$ vs. CTRL 24 h; ****$p < 0.0001$ vs. CTRL 72 h by one-way ANOVA. (**c**) The relative percentage increase or decrease in hCECs number was measured at 24 h and 72 h in cells cultured 2 mg/ml dECM hydrogel with or without 10 nM NAP. The bar graphs show quantitative analysis obtained by three independent experiments. Data represent means ± SEM. **$p < 0.01$ vs. CTRL 24 h by one-way ANOVA.

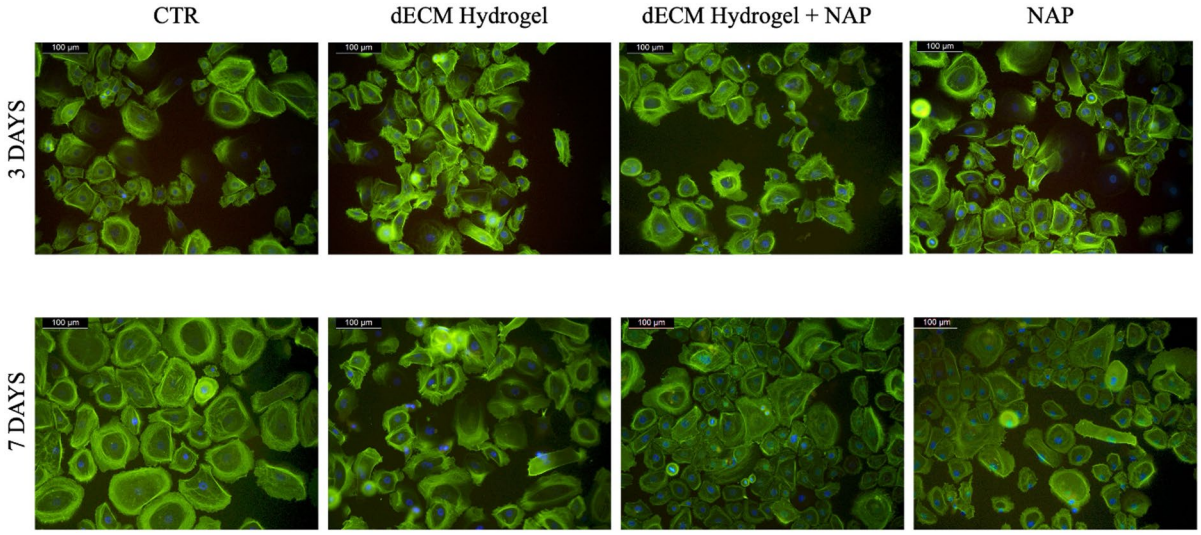

Fig. 3. Morphological evaluation of PCs cells after 3 and 7 days of culture with dECM hydrogel with or without NAP. To determine the phenotype, morphology, and general condition of the cells, PCs cells were stained with Fluorescein Phalloidin (green) staining. Nuclei were stained with DAPI (blue). Images represent control cells, and cells cultured onto surfaces previously coated with dECM hydrogel, or NAP, or dECM hydrogel-NAP. Images are representative of all results obtained in the three different experiments. Scale bar = 100 µm.

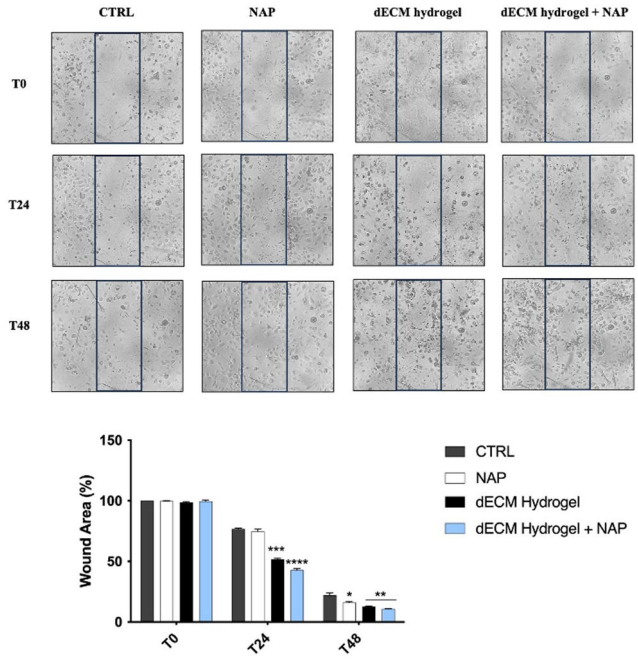

Fig. 4. dECM hydrogel promotes wound closure in hCECs. Representative images of wound healing assays performed in hCECs onto surfaces previously coated with dECM hydrogel, or NAP, or dECM hydrogel-NAP at 0, 24, and 48 h. The bar graph shows the average wound area expressed in the percentage of CTRL. Data are shown as mean ± SD (from $n = 3$ independent experiments). ***$p < 0.001$ and ****$p < 0.0001$ vs. CTRL 24 h; *$p < 0.05$, **$p < 0.01$ vs. CTRL 48 h by one-way ANOVA.

presence of dECM hydrogel-NAP (***$p < 0.001$ and ****$p < 0.0001$). SIRC cells showed a significant reduction of wound area when seeded in dECM hydrogel-NAP (****$p < 0.0001$) (Supplementary Fig. 3). At 48 h, a significant reduction in wound area was observed in the presence of NAP or dECM hydrogel, but the greatest effect was observed in the presence of dECM hydrogel-NAP for both cell lines (**$p < 0.01$ and ****$p < 0.0001$) (Fig. 4 and Supplementary Fig. 2). Although we did not perform experiments to verify whether scratching with the 200 µL

pipette tip compromised the integrity of the dECM hydrogel in the wound area, the results demonstrated that the hydrogel promoted wound repair, and its support was essential for effective wound healing.

The regenerative potential of dECM hydrogel with or without NAP, was also investigated in PCs cells, that were seeded in 96-well plates at a density of 10 000 cells/well to create a confluent monolayer. Twenty-four hours after cell plating, the IncuCyte WoundMaker device was used to create a homogeneous scratch wound in each well of the 96-well plate. Images were analyzed using the IncuCyte Zoom Scratch Wound analysis module measuring the relative wound confluence over time. As shown in Supplementary Fig. 3, the dECM with or without NAP seemed to slightly increase the ability of the PCs to migrate into the wound site of the scratch wound assays, nevertheless none of the results have a significant effect on PCs migration.

dECM hydrogel-NAP preserves 3D organotypic corneal epithelium barrier against high glucose (HG)-induced damage

To investigate the possible effect of dECM hydrogel-NAP on DK, a 3D organotypic corneal epithelium model, through the ALI culture system (Fig. 5a), was first constructed. As shown in Figs. 3D and 5b organotypic corneal epithelium displays a similar morphology to human corneal epithelium in vivo. Moreover, immunohistochemical (IHC) analysis showed positive staining for cytokeratin 3 (CK3) and cytokeratin 15 (CK15), which represent typical markers of human corneal epithelium[25,26]. No CD34 staining was detected, confirming the purity of our model (Fig. 5b).

Next, to reproduce the DK model, the 3D organotypic corneal epithelium was cultured in high glucose (HG) levels (25 mM), alone or in the presence of dECM hydrogel-NAP (Fig. 5c). As shown in Fig. 5d, the 3D organotypic corneal epithelium cultured in HG, showed a strong reduction in the number of layers, as compared to the epithelial corneal barrier cultured under normal glucose condition and consequently a decreased expression of the specific epithelial marker CK3. Noteworthy, dECM hydrogel-NAP supported the phenotype of 3D organotypic corneal epithelium grown under HG, as demonstrated by restored corneal epithelium barrier in terms of number of layers and CK3 expression.

Morphological evidence was corroborated by the analysis of the thickness of the 3D corneal epithelium. As shown in Fig. 6a, the thickness of the 3D corneal epithelium barrier was strongly reduced in the HG group,

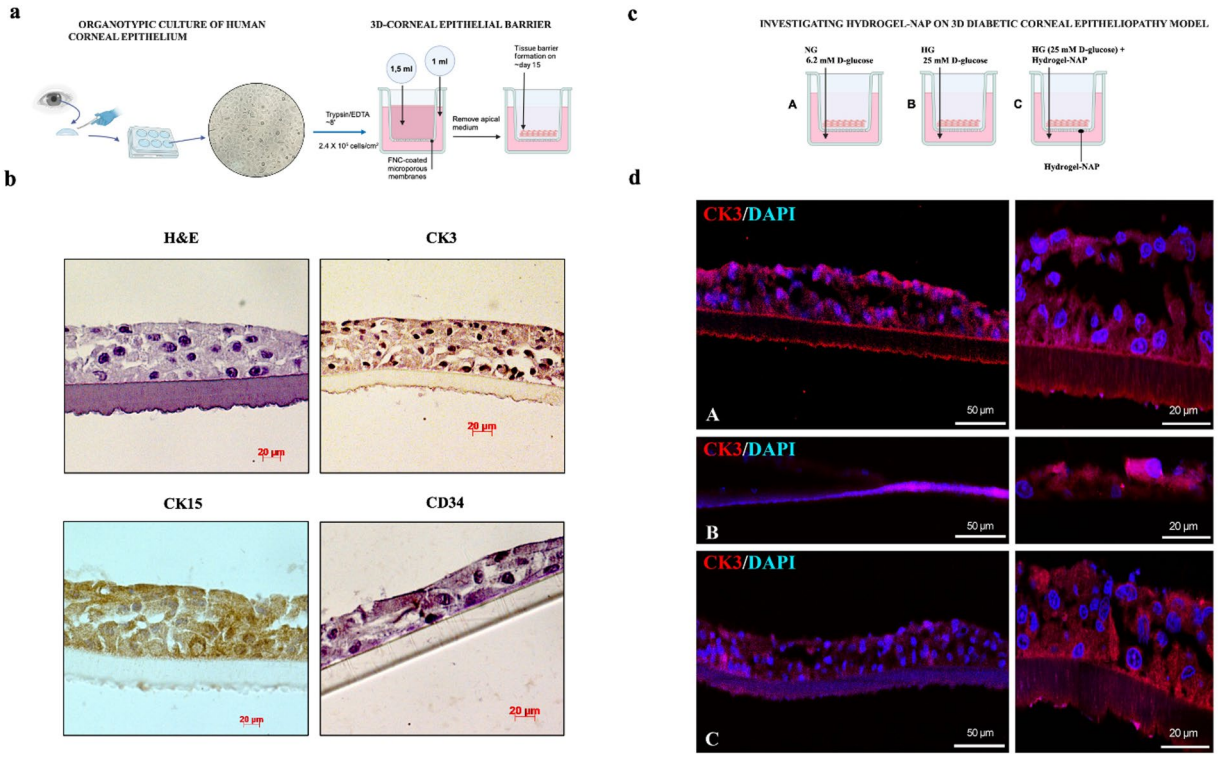

Fig. 5. Realization and characterization of 3D organotypic corneal epithelium. (**a**) Graphical overview of the workflow. (**b**) Representative hematoxylin-eosin (H&E) and immunohistochemical (IHC) staining of CK3, CK15 and CD34 in ALI tissue at 15 days. Digital micrographs are representative results of fields taken in randomly selected slides and obtained using the Zeiss Axioplan light microscope (Carl Zeiss) fitted with a digital camera (AxioCam MRc5; Carl Zeiss). Scale bars, 20 µm, magnification 400x. (**c**) ALI tissue cultured under high glucose (25 mM) levels to mimic aqueous humor glucose levels in patients with DK. (**d**) CK3 signal (red fluorescence) was detected in 3D organotypic corneal epithelium cultured in NG (A), or in HG (B) or in HG onto surfaces previously coated with dECM hydrogel-NAP (C). Cell nuclei were stained with DAPI (blue fluorescence). The photomicrographs are representative results taken from different fields in randomly selected slides and scanned by confocal laser scanning microscopy (CLSM). Scale bars, 50 µm and 20 µm.

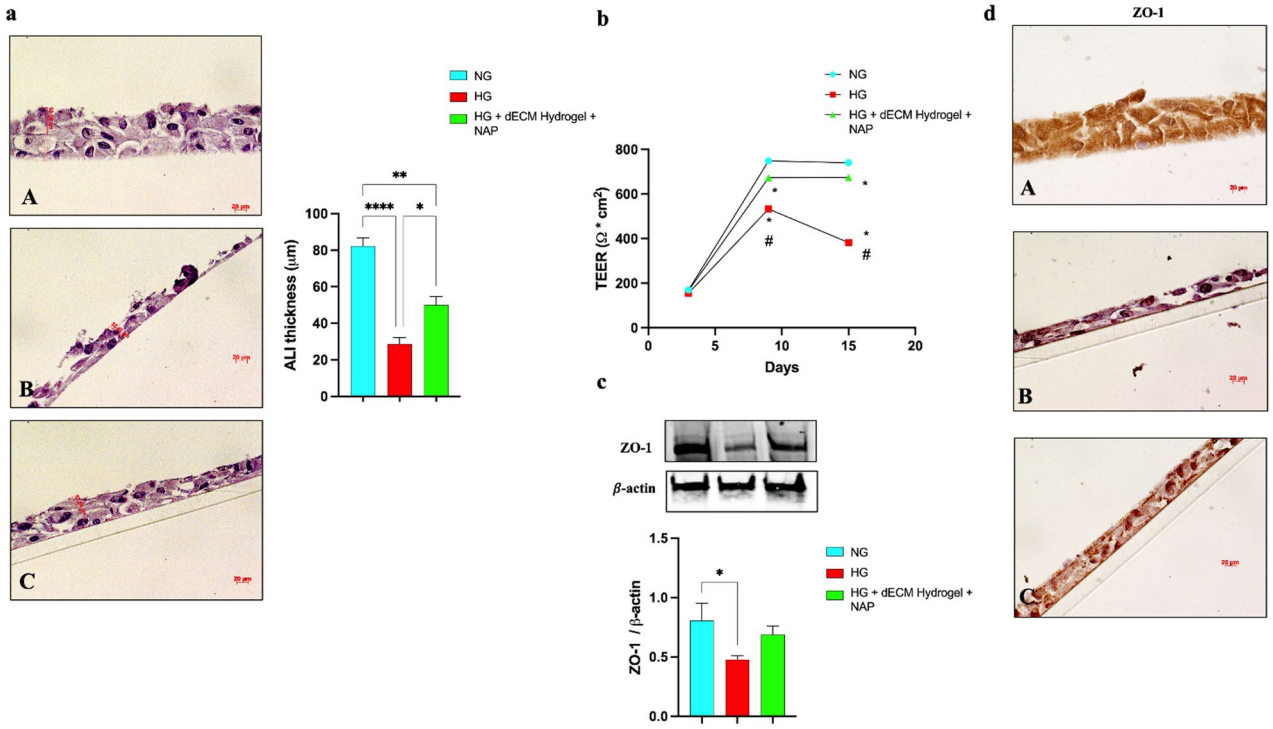

Fig. 6. dECM hydrogel-NAP counteracts HG induced-corneal epithelium barrier damage. (**a**) H&E at 15 days of 3D corneal epithelium cultured on NG (A), or in HG (B) or in HG onto surfaces previously coated with dECM hydrogel-NAP (C). Digital micrographs are representative results of fields taken in randomly selected slides and obtained using the Zeiss Axioplan light microscope (Carl Zeiss) fitted with a digital camera (AxioCam MRc5; Carl Zeiss). Scale bars, 20 μm, magnification 400x. The bar graph shows ALI thickness measured at 15 days. Data resulting from three independent experiments are represented as means ± SEM. $^{*}p < 0.05$ vs. HG, $^{**}p < 0.01$ and $^{****}p < 0.0001$ vs. NG by one-way ANOVA. (**b**) TEER expressed in Ω·cm2, was evaluated on 3D corneal epithelium cultured on NG or HG, or in HG onto surfaces previously coated with dECM hydrogel-NAP, at days 3, 9 and 15. Data resulting from three independent experiments are represented as means ± SEM. $^{*}p < 0.05$ vs. NG and $\#p < 0.05$ vs. HG + Hydro-NAP by one-way ANOVA. (**c**) Representative immunoblots of ZO-1 expression in hCECs cultured under NG, or HG, or in HG onto surfaces previously coated with dECM hydrogel-NAP. The bar graphs show quantitative analysis obtained by three independent experiments. Data are presented as the mean ± SEM. $^{*}p < 0.05$ vs. NG by one-way ANOVA. Relative band densities were quantified by using ImageJ software. Protein levels are expressed as arbitrary units obtained following normalization to β-actin, which was used as loading control. The original blots/gels are presented in Supplementary Fig. 4. (**d**) Staining for the ZO-1 marker in ALI tissue cultured on NG (A), or in HG (B) or in HG onto surfaces previously coated with dECM hydrogel-NAP (C). Digital micrographs are representative results of fields taken in randomly selected slides and obtained using the Zeiss Axioplan light microscope (Carl Zeiss) fitted with a digital camera (AxioCam MRc5; Carl Zeiss). Scale bars, 20 μm, magnification 400x.

compared to the normal glucose (NG) group ($^{****}p < 0.0001$). The dECM hydrogel-NAP counteracted the HG microenvironment-induced effect, as demonstrated by the increase of barrier thickness as compared to the HG group ($^{*}p < 0.5$). The positive role played by the dECM hydrogel-NAP was also confirmed through transepithelial electrical resistance (TEER) analysis, which allowed us to monitor barrier tissue development, formation, and functional maturation. As shown in Fig. 6b, on day 15, the TEER values of the NG group were ~740 Ω·cm², which are comparable to those reported in human studies, where the mean corneal TEER was 690 ± 69 Ω·cm²[27]. High glucose levels inhibited the proper development of the corneal epithelial barrier, as demonstrated by the low TEER levels measured on day 9 (~ 530 Ω*cm²) and day 15 (~ 380 Ω*cm²) as compared to the TEER values of the NG group ($p < 0.0001$). On the contrary, higher TEER values (day 9 and day 15: ~670 Ω*cm2) were measured on 3D corneal barrier cultured under HG and in the presence of the dECM hydrogel-NAP. We also evaluated the expression and distribution of zonula occludens (ZO)−1, which is localized in superficial and sub-superficial cell layers of the corneal epithelium, contributing to the barrier function. As shown in Fig. 6c, ZO-1 expression is drastically decreased in hCECs cultured under HG levels ($^{*}p < 0.05$). Whereas, ZO-1 expression levels were restored in the HG + dECM hydrogel-NAP group. Moreover, as shown by IHC analysis (Fig. 6d), in NG and HG + dECM hydrogel-NAP groups, high-intensity levels of ZO-1 were detected throughout the various corneal epithelial layers. Exposure of the 3D organotypic corneal epithelium to HG levels drastically affected ZO-1 pattern distribution. This data supports the idea that the dECM hydrogel-NAP helps the corneal epithelium to regain its organized structure, counteracting HG-induced damage.

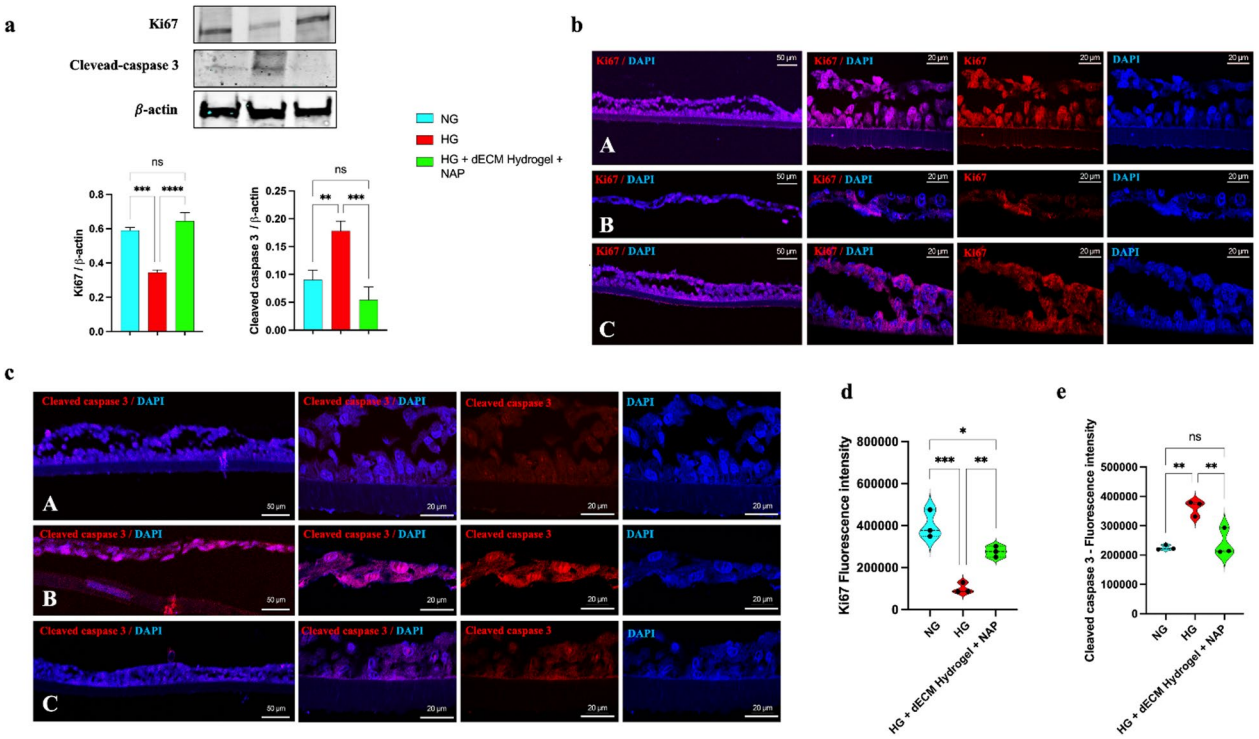

Fig. 7. dECM hydrogel-NAP attenuates apoptosis and sustains proliferation of 3D corneal epithelium in DK model. (**a**) Representative immunoblots of Ki67 and Cleaved-caspase 3 expression in hCECs cultured under NG, or HG, or in HG onto surfaces previously coated with dECM hydrogel-NAP. The bar graphs show quantitative analysis obtained by three independent experiments. Data are presented as the mean ± SEM. $^{**}p < 0.01$ and $^{***}p < 0.001$ vs. NG; $^{***}p < 0.001$ and $^{****}p < 0.0001$ vs. HG by one-way ANOVA. Relative band densities were quantified by using ImageJ software. Protein levels are expressed as arbitrary units obtained following normalization to β-actin, which was used as loading control. The original blots/gels are presented in Supplementary Fig. 4. (**b**-**c**) Ki67 and Cleaved-caspase 3 signal (red fluorescence) were detected in 3D organotypic corneal epithelium cultured in NG (A), or in HG (B) or in HG onto surfaces previously coated with dECM hydrogel-NAP (C). Cell nuclei were stained with DAPI (blue fluorescence). The photomicrographs are representative results taken from different fields in randomly selected slides and scanned by confocal laser scanning microscopy (CLSM). Scale bars, 50 µm and 20 µm. (**d**-**e**) Fluorescence intensities were obtained with the "Profile view" function of ZEN-2011 software; the fluorescence red was read for each pixel along the line, and the violin plots reflect, in arbitrary units, the proportion of the pixel intensity in the wavelength. Data represent means ± SEM (from $n = 3$ independent experiments). $^{*}p < 0.05$, $^{**}p < 0.01$ and $^{***}p < 0.001$ vs. NG; $^{**}p < 0.01$ vs. HG by one-way ANOVA.

dECM hydrogel-NAP attenuates apoptosis of 3D corneal epithelium in DK model

We have provided evidence that 3D organotypic corneal epithelial barrier cultured in the presence of dECM hydrogel-NAP are largely maintained even under a high-glucose environment. Therefore, we analyzed its effect against apoptotic cell death induced by HG. As shown in Fig. 7a, exposure to elevated glucose caused reduced proliferation marker Ki67 expression levels and increased pro-apoptotic marker cleaved caspase-3 expression (Fig. 7a). Noteworthy, 3D organotypic corneal epithelium cultured under high glucose in the presence of dECM hydrogel-NAP showed inverted results, with significantly increased and decreased Ki67 and cleaved caspase-3 levels, respectively.

In addition, through confocal microscopy, we assessed that the expression of the proliferation marker Ki67, strongly expressed in the entire epithelium and in particular in the basal epithelium of normal glucose conditions, was drastically reduced in the HG group. As expected, the 3D culture, grown on dECM hydrogel-NAP, showed restoration of Ki67 expression (Fig. 7b). In the diabetic-mimetic 3D corneal epithelium, many cleaved caspase-positive cells were observed across the entire epithelium (Fig. 7c). Conversely, barely any cleaved caspase 3-positive cells were observed in the HG + dECM hydrogel-NAP group (Fig. 7c). That is, the dECM hydrogel-NAP treatment markedly reversed the apoptotic response. Taken together, these results suggested that dECM hydrogel-NAP can counteract apoptosis of corneal epithelium during DK and more rapidly regenerate the epithelium.

Discussion

Diabetes mellitus is associated with systemic morbidities among the human population. Progressive damage occurs in major end-organs. However, the most superficial organ affected by diabetes is the cornea. All the

corneal components, epithelium, nerves, immune cells, and endothelium, are affected by diabetes. The corneal epithelium consists of keratocytes linked by tight junctional complexes, residing in an ECM predominantly made of type 1 collagen. The corneal epithelium is constantly exposed to wear and tear and needs to be regenerated. At the ocular surface, the loss of innervation and trophic support reduces the corneal sensitivity, induces apoptosis, and is associated with reduction of lacrimal production, inducing persistent epithelial defects and impaired wound healing function[28]. Disruption of tight junctional complexes, loss of basal corneal epithelial cells with changes in epithelium thickness and stroma cause corneal opacification, affecting light transmission and vision[2]. While corneal denervation and diabetic retinopathy are targets of early metabolic and microvascular disease, diabetic keratopathy and impaired corneal epithelial wound healing appear at a later stage, implying a widespread disease[2]. Restoration of corneal epithelial homeostasis and the associated corneal nerve plexus challenge the conventional therapies, due to the anatomical and functional complexities. Considering the global shortage of donor, corneal tissue engineering introduced the potential of hydrogel-based materials, which have been identified as promising tools for drug delivery and tissue repair. It is well known that the use of natural hydrogels (e.g., collagen, gelatin, hyaluronic acid and alginate) and synthetic materials, such as polyethylene glycol (PEG) and polyvinyl alcohol (PVA), on epithelial cells demonstrated to have high adhesion, proliferation and migration, which are vital processes for corneal repair during wound healing. Moreover, the natural materials, contain collagen and hyaluronic acid which support epithelialization, minimize inflammation and fibrosis to establish an ideal healing environment. In this context, the hydrogels derived from decellularized extracellular matrix (dECM) hold great promises in corneal tissue engineering[29]. In fact, the preserved matrix contains essential components including collagens, glycosaminoglycans (GAGs), laminin and fibronectin which create a highly bioactive environment that closely resembles the native corneal microenvironment and tissue-specific regeneration. These hydrogels can be engineered and tailored in a tissue-specific manner, providing both mechanical compliance while creating a bioactive biochemical environment, allowing cells to adhere, migrate and proliferate[30]. Although several corneal applications of hydrogels exist, they remain in an early phase of development[31]. Our functionalized dECM biomaterial is based on the idea that both the lamellar ECM and keratocytes health contributes significantly to the cornea's transparency and function[12]. The dECM hydrogel is biocompatible to corneal cells, maintains the transparency and allows the functionalization with NAP peptide, which in turn has been shown to have protective effects in the eye[15]. In particular, in corneal epithelium exposed to UV-B radiation, NAP has been shown to reduce reactive oxygen species formation by indirectly inhibiting the c-Jun N-terminal Kinase (JNK)/Bax signaling pathway[18]. In the same model, the treatment with NAP showed to counteract the expression of inflammatory cytokines in corneal epithelial cells, affecting nuclear factor-κB (NF-κB) activation[17]. Considering that reactive oxygen species (ROS) generation, resulting in the activation of JNK pathway and NF-κB activation, represents key elements involved in the pathogenesis of DK[5,32], the protective effects of NAP may be ascribed to these ways. By mitigating oxidative stress and suppressing pro-inflammatory signaling cascades, including the JNK/Bax and NF-κB pathways, NAP may help preserve corneal integrity in diabetic conditions. Furthermore, the modulation of these pathways suggests a broader cytoprotective role, potentially reducing apoptosis and maintaining epithelial barrier function.

In this work, the application of dECM hydrogel-NAP was tested on human and rabbit corneal epithelial cells and in a 3D-organotypic corneal epithelium model with hCECs derived from donor cornea that closely mimic the morphology and function of the native corneal epithelium. Upon high glucose levels, to reproduce the DK microenvironment, the 3D-organotypic corneal epithelium showed clinically relevant disease hallmarks, including increased apoptosis and consequently corneal epithelium barrier alterations, in terms of resistance and reduced expression of ZO-1. Consistent with our findings, in vitro and in vivo studies showed alteration of tight junction complexes expression in DK, leading to delayed wound healing, epithelial defects, corneal infections, and other complications[8,33]. Our results showed that the application of dECM hydrogel restored the corneal epithelium architecture, with the enhancement of the effects in the presence of NAP functionalization.

Our study has some limitations. Light transmittance was evaluated only at a single representative wavelength (595 nm). While this wavelength corresponds to the peak transmittance of the human cornea and is a reliable indicator of clinical opacity, a full spectral analysis was not performed. Future studies will include measurements across the entire visible spectrum (400–800 nm) to provide a more comprehensive optical characterization of the hydrogels. Although our model accurately replicates the corneal epithelium barrier, it lacks incorporation of the tear film and eyelid mechanics, as well as corneal innervation. Moreover, an investigation on the role of dECM hydrogel-NAP against the oxidative stress and inflammatory process characterized DK is necessary. Therefore, future research will test the anti-oxidant and anti-inflammatory effects of dCEM hydrogel-NAP on a full-thickness 3D organotypic cornea to address these limitations. Moreover, the use of cornea-on-a-chip can reproduce the interaction with the aqueous humor and tear fluid.

In conclusion, we examined the efficacy of a novel dECM hydrogel functionalized with NAP on a 3D organotypic human corneal epithelium model exposed to high glucose levels mimicking conditions of DK. We successfully reproduce essential characteristics of DK, such as disrupted epithelial structure and increased apoptotic cells death. Interestingly, dECM hydrogel-NAP counteracts the cascade of events involving disrupted cellular structure, and altered cellular viability, fostering the advancements for in-vivo preclinical studies. Overall, the dECM hydrogel-NAP has several potential applications, including topical treatment, bioactive contact lenses coated with or embedded with the dECM hydrogel-neuropeptide formulation and/or post-surgical therapy to enhance recovery in diabetic patients undergoing corneal procedures.

Materials and methods

Ethics statement

This study was performed according to the tenets of the Declaration of Helsinki. The sclerocorneal button stored in organ culture at 31° C were provided for penetrating keratoplasty by the Eye Bank, Fondazione Banca degli

Occhi del Veneto (Venezia-Mestre, Italy), which obtained informed consent for all tissue samples held and cultured (Ethical approval was granted on 19 February 2024; number 09/2024/PAR by the Institutional Review Board of the University of Catania).

Decellularization of the bovine pericardial extracellular matrix

Hydrogel was derived from bovine pericardium extracellular matrix (dECM) through a decellularization process developed by Tissuegraft Srl (Alessandria, Italy) (Italian Patent: 102020000007567, International Patent: PCT/IB2021/052779). The decellularization method, validated by Tissuegraft, effectively removed cellular components while preserving the ECM essential protein content. The dECM liquid hydrogel alone or in combination with 10 nM NAP (New England Peptide, MA, USA) at a final concentration of 2 mg/ml was finally used for cytocompatibility and regenerative potential testing. In all experiments, the surfaces were coated with 50 µL/cm^2 of dECM hydrogel.

Optical characterization

dECM hydrogels at different concentrations (9 mg/ml, 4 mg/ml 2 mg/ml and 2 mg/ml with NAP) were prepared in 96 well plate in triplicate and transmittance to visible light (595 nm) was assessed using Victor4X Multilabel Plate Reader (Perkin Elmer, Milan, Italy), phosphate buffered saline (PBS) was used as blank. The obtained absorbance values were converted to transmittance by Beer Lambert's law. Mean transmittance was derived by averaging the values obtained. Moreover, in order to assess the transparency over time, transmittance was observed up to two weeks at different hydrogel concentrations.

Cell cultures

Human corneal epithelial cells (hCECs) were obtained from donor corneas [$n = 5$] as previously described[34,35]. Briefly, triangular-shaped pieces from donor corneas were placed epithelial side down, in a six-well plate, previously treated with fibronectin (FNC Coating Mix, Catalog Number: 0407, Baltimore, USA), and cultured for 24 h with a drop of antibiotics-free culture medium (PCS-700-030, ATCC, USA), containing corneal epithelial growth factor (PCS-700-040, ATCC) at 37 °C in a humidified atmosphere of 95% air and 5% CO^2. The next day, 1 ml of medium was added to each well, and the day 5, the corneal pieces were removed. At 80% confluence, cells were split and seeded in T25 flasks previously treated with fibronectin.

Statens Seruminstitut rabbit corneal (SIRC) epithelial cells (ATCC CCL-60) were cultured in 75 cm^2 flasks, and grown in Eagle's Minimum Essential Medium (ATCC® 30–2003TM) supplemented with 10% fetal bovine serum (FBS, 10108–165, GIBCO, Milan, Italy).

Primary human corneal epithelial cells (PCs) (ATCC PCS-700-010, LGC Standards, Italy) were cultured in 75 cm^2 flasks and grown in Corneal Epithelial Cell Basal Medium (PCS-700-030, ATCC) supplemented with Corneal Epithelial Cell Growth Kit (PCS-700-040, ATCC) following the manufacturer instructions. Cells were seeded at density of 1×10^4 at cm^2.

Cell viability assay

The relative percentage increase or decrease in cell number was assessed using 3-[4,5-dimethylthiazol-2-yl]−2,5-diphenyltetrazolium bromide salt (MTT) (Sigma-Aldrich), as previously described[36]. Briefly, hCECs and SIRC cells were seeded at a density of 1×10^4 cells/well in 100 µL of culture medium for 24 h and 72 h in 96-well plates coated with 16,5 µL of different dECM hydrogel concentrations. Then the medium was replaced with a fresh medium with MTT salt added to each well for 3 h. Finally, dimethyl sulfoxide (DMSO) was used to dissolve formazan salts, and absorbance was measured at 570 nm in a plate reader (VariosKan, Thermo Fisher Scientific, Waltham, MA, USA). Six replicate wells were used for each group. The medium alone was used as a blank.

Lactate dehydrogenase (LDH) release assay

The extracellular LDH activity was evaluated by using the CyQUANT LDH Cytotoxicity Assay (Thermo Fisher Scientific). Briefly, hCECs and SIRC cells were seeded at 1×10^4 cells/well in 100 µL of culture medium for 24 h and 72 h in 96-well plates coated with 16,5 µL of different dECM hydrogel concentrations. Then, 50 µL of medium was transferred into a new 96-well plate, and 50 µL of working solution was added. After 30 min at room temperature, 50 µL of stop solution was added. A Varioskan microplate reader was used to measure the absorbance values at 490 nm. LDH release was documented as LDH (% control) as follows: $(abs_x \div abs_{ctrl+}) \times 100$, where abs_x is the absorbance in the x well, and abs_{ctrl+} is the average absorbance of internal positive control cells (untreated lysed cells). Absorbance values were edited by removing blanks.

Wound-healing assay

hCECs and SIRC cells were cultured in six-well dishes (5×10^4 cells/well) coated with 450 µL of dECM hydrogel at a final concentration of 2 mg/mL alone or in combination with 10 nM NAP. After reaching the confluence, they were scratched with a 200 µL pipette tip. Each well was washed with PBS solution. Then, the cells were cultured in culture medium. Wound area was analyzed from six different wells for each treatment, and all images were acquired with a Leica microscope using a ×100 magnification. The average wound area, expressed in the percentage of control (CTRL), was determined using ImageJ Software (Broken Symmetry Software, Bethesda, MD, United States)[37].

The Wound-Healing Assay was also performed on PCs and imaged using the IncuCyte Zoom Live Cell Imaging System and Scratch Wound analysis module per the manufacturer's instructions (IncuCyte, Sartorius). Briefly, PCs cells were seeded in 96-well plates pre-coated (2 mg/ml dECM hydrogel with and without NAP) at a final density of 10 000 cells/well. The following day, scratch wounds were performed using the IncuCyte WoundMaker following the manufacturer's instructions (IncuCyte, Sartorius). The media was then replaced

to remove cell debris, and the plate was imaged every 4 h using the IncuCyte for 24 h. Wound closure was calculated using IncuCyte's wound confluence analysis module for each image over time.

3D organotypic corneal epithelium tissue

To generate 3D organotypic corneal epithelium, hCECs were cultured (2.4×10^5 cells/cm^2) in transwell inserts with FNC-precoated polycarbonate membrane with pore size 0.4 μm (CLS3401, Meck, Darmstadt, Germany) as previously described[38]. Antibiotics-free medium with growth factors was added both in the bottom and the apical part. The day after, the medium in the apical part was removed and cells were cultured in air-liquid interface (ALI) to generate 3D organotypic corneal epithelium. The medium was changed every 3 days up to the 15th day.

Diabetic keratopathy model condition

The 3D organotypic corneal epithelium was cultured under high glucose levels based to literature-reported in vitro models of diabetic keratopathy[8,39,40]. In particular, cells were cultured in culture medium (PCS-700-030) contains 6.2 mM glucose representing the control group (normal glucose, NG), or in the presence of 18.8 mM glucose to reach a final concentration of 25 mM glucose (high glucose, HG). Mannitol (18.8 mM) was used in NG group as an osmotic control.

Histological and immunohistochemical characterization

The 3D organotypic corneal epithelium tissues were fixed in 10% formalin for 24 h, dehydrated in graded ethanol, and paraffin-embedded. The histological analysis was made on 5 μm sections obtained through a rotary manual microtome (Leica RM2235, Milan, Italy). Cellular and tissue structures were viewed by hematoxylin and eosin staining.

The expression and distribution of CK3, CK15, CD34 and ZO-1 in histological sections from 3D organotypic corneal epithelium was analyzed through immunohistochemistry using the following primary antibodies: anti-cytokeratin 3 (CK3) (3850-MSM1, NeoBiotechnologies, USA); anti-cytokeratin 15 (CK15) (cat. no. MA1-90929, Invitrogen); anti-CD34 (cat. No. PA5-89536, Invitrogen); anti-ZO-1 (cat. no. 61–7300, Thermo Fisher, MA, USA), diluted in phosphate-buffered saline (PBS) and 1% bovine serum albumin (BSA). The immunoreaction was observed using a 3,3′-diaminobenzidine solution (DAB substrate, D7304, Sigma-Aldrich, USA). The samples were lightly counterstained with hematoxylin mounted in the vecta mount (Vector Laboratories).

The sections were examined using a Zeiss Axioplan light microscope (Carl Zeiss, Oberkochen, Germany) and the pictures were acquired with a digital camera (AxioCam MRc5, Carl Zeiss, Oberkochen, Germany).

Measurement of epithelial layer thickness

The 3D organotypic corneal epithelial layer thickness at day 15 was determined on sections stained with hematoxylin and eosin. The thickness of the epithelium at three positions per image in up to three images per experiment was measured by using ImageJ software (NIH, Bethesda, MD; available at http://rsb.info.nih.gov/ij/index.html, accessed on 5 May 2025).

Transepithelial electrical resistance

Transepithelial electrical resistance (TEER) of 3D organotypic corneal epithelium was measured by using a Millicel-Electrical Resistance System (ERS2, Millipore, Epithelial Volt-Ohm Meter)[41]. Values are expressed as Ω·cm^2. The combined resistance of the filter was subtracted from the values of filter cultured organotypic ALI 3D to calculate the resistance of the corneal epithelium barrier. Measurements were performed at days 3, 9 and 15, in three different wells for each experimental condition.

Western blot analysis

About 30 μg of proteins, extracted from total cell lysate with RIPA homogenizer, were loaded on 4–12% tris–glycine gel. Membranes were incubated overnight (4 ∘C) with specific primary antibodies: anti-ZO-1 (cat. no. 61–7300, Thermo Fisher, MA, USA); anti-cleaved caspase 3 (#9661, Cell Signaling Technology); anti-Ki-67 (30 – 9) (cat. no. 790–4286, Roche); anti- β-actin (C4) (SC-47778, Santa Cruz Biotechnology). The secondary antibody, goat anti-rabbit IRDye 800CW (926–32211; Li-Cor Biosciences) and goat anti-mouse IRDye 680CW (926-68020D; Li-Cor Biosciences), was used at 1:20,000. Blots were scanned with an Odyssey Infrared Imaging System (Odyssey, Li-Cor Biosciences, Lincoln, NE, USA) as previously described[42]. ImageJ software was used for the densitometric analyses of Western blot signals. Values were normalized to β-actin used as a loading controls.

Immunofluorescence analysis

PCS cells were seeded onto pre-coated (50 μL/cm^2 of 2 mg/ml dECM hydrogel with and without NAP) glass coverslips. After 7 days, cells were fixed with 4% formalin in PBS (pH 7.4), rinsed and stained with phalloidin (Sigma Aldrich, Milan, Italy) and with 300 nM Diamidine-20-phenylindole dihydrochloride (DAPI) (Sigma Aldrich, Milan, Italy) for the nuclei dye. A final rinsing was done before the samples were mounted (60% glycerol in PBS) onto glass slides and observed. Representative images were taken with the fluorescence Leica DM2500 microscope (Wetzlar, Germany) and acquired via Leica software.

To evaluate in ALI tissue the cellular distribution of CK3, Cleaved caspase-3 and Ki67, immunofluorescence analysis was performed as previously described[40]. The sections were incubated overnight at 4 ∘C with the specific antibodies: anti-CK3 (3850-MSM1, NeoBiotechnologies); anti-cleaved caspase 3 (#9661, Cell Signaling Technology) and anti-Ki67 (30 – 9) (cat. no. 790–4286, Roche). Signals were revealed with Alexa Fluor 488 goat anti-mouse and Alexa Fluor 594 goat anti-rabbit, for 1.5 h at room temperature (shielded from light). DNA was counter-stained with 4,6-diamidino-2-phenylindole (DAPI; cat. no 940110; Vector Laboratories,

Burlingame, CA, USA). Immunolocalization was analyzed by confocal laser scanning microscopy (Zeiss LSM700, Oberkochen, Germany).

Statistical analysis

Data are represented as the mean ± standard error of the mean. One-way analysis of variance was used to compare the means between two or more groups, and statistical significance was assessed by the Tukey–Kramer post hoc test. The level of significance for all statistical tests was set at $p \leq 0.05$. Data were analyzed using GraphPad Prism 9 (GraphPad Software, La Jolla, CA, USA).

Data availability

Data is provided within the manuscript or supplementary information files.

Received: 23 July 2025; Accepted: 12 January 2026
Published online: 14 January 2026

References

1. Hossain, M. J., Al-Mamun, M. & Islam, M. R. Diabetes mellitus, the fastest growing global public health concern: Early detection should be focused. *Health Sci Rep* **7**, e2004. https://doi.org/10.1002/hsr2.2004 (2024).
2. Shih, K. C., Lam, K. S. & Tong, L. A systematic review on the impact of diabetes mellitus on the ocular surface. *Nutr Diabetes* **7**, e251. https://doi.org/10.1038/nutd.2017.4 (2017).
3. Zhang, J., Wang, M., Chen, L. & Radke, N. Diabetic Blindness Remains a Big Challenge Despite All Recent Advancements in Diagnostics and Treatments. *Asia Pac J Ophthalmol (Phila)* **13**, 100105, https://doi.org/10.1016/j.apjo.2024.100105 (2024).
4. Priyadarsini, S. et al. Diabetic keratopathy: Insights and challenges. *Surv Ophthalmol* **65**, 513–529. https://doi.org/10.1016/j.survophthal.2020.02.005 (2020).
5. Zhao, H., He, Y., Ren, Y. R. & Chen, B. H. Corneal alteration and pathogenesis in diabetes mellitus. *Int J Ophthalmol* **12**, 1939–1950. https://doi.org/10.18240/ijo.2019.12.17 (2019).
6. Kim, Y. J. & Kim, T. G. The effects of type 2 diabetes mellitus on the corneal endothelium and central corneal thickness. *Sci Rep* **11**, 8324. https://doi.org/10.1038/s41598-021-87896-3 (2021).
7. Buonfiglio, F., Wasielica-Poslednik, J., Pfeiffer, N. & Gericke, A. Diabetic Keratopathy: Redox Signaling Pathways and Therapeutic Prospects. *Antioxidants (Basel)* **13**, https://doi.org/10.3390/antiox13010120 (2024).
8. Jiang, Q. W. et al. Diabetes inhibits corneal epithelial cell migration and tight junction formation in mice and human via increasing ROS and impairing Akt signaling. *Acta Pharmacol Sin* **40**, 1205–1211. https://doi.org/10.1038/s41401-019-0223-y (2019).
9. Brown, M., Li, J., Moraes, C., Tabrizian, M. & Li-Jessen, N. Y. K. Decellularized extracellular matrix: New promising and challenging biomaterials for regenerative medicine. *Biomaterials* **289**, 121786. https://doi.org/10.1016/j.biomaterials.2022.121786 (2022).
10. Di Francesco, D. *et al.* Regenerative Potential of A Bovine ECM-Derived Hydrogel for Biomedical Applications. *Biomolecules* **12**, https://doi.org/10.3390/biom12091222 (2022).
11. Chameettachal, S. et al. Human cornea-derived extracellular matrix hydrogel for prevention of post-traumatic corneal scarring: A translational approach. *Acta Biomater* **171**, 289–307. https://doi.org/10.1016/j.actbio.2023.09.002 (2023).
12. Di Francesco, D. et al. Characterization of a decellularized pericardium extracellular matrix hydrogel for regenerative medicine: insights on animal-to-animal variability. *Front Bioeng Biotechnol* **12**, 1452965. https://doi.org/10.3389/fbioe.2024.1452965 (2024).
13. Morimoto, B. H., Fox, A. W., Stewart, A. J. & Gold, M. Davunetide: a review of safety and efficacy data with a focus on neurodegenerative diseases. *Expert Rev Clin Pharmacol* **6**, 483–502. https://doi.org/10.1586/17512433.2013.827403 (2013).
14. Galushkin, A. & Gozes, I. Intranasal NAP (Davunetide): Neuroprotection and circadian rhythmicity. *Adv Drug Deliv Rev* **220**, 115573. https://doi.org/10.1016/j.addr.2025.115573 (2025).
15. Maugeri, G., D'Amico, A. G., Magrì, B., Musumeci, G. & D'Agata, V. Activity-Dependent Neuroprotective Protein (ADNP): An Overview of Its Role in the Eye. *Int J Mol Sci* **23**, https://doi.org/10.3390/ijms232113654 (2022).
16. Jehle, T. et al. The neuropeptide NAP provides neuroprotection against retinal ganglion cell damage after retinal ischemia and optic nerve crush. *Graefes Arch Clin Exp Ophthalmol* **246**, 1255–1263. https://doi.org/10.1007/s00417-007-0746-7 (2008).
17. Maugeri, G. *et al.* Regulation of UV-B-Induced Inflammatory Mediators by Activity-Dependent Neuroprotective Protein (ADNP)-Derived Peptide (NAP) in Corneal Epithelium. *Int J Mol Sci* **24**, https://doi.org/10.3390/ijms24086895 (2023).
18. Maugeri, G. *et al.* Activity-Dependent Neuroprotective Protein (ADNP)-Derived Peptide (NAP) Counteracts UV-B Radiation-Induced ROS Formation in Corneal Epithelium. *Antioxidants (Basel)* **11**, https://doi.org/10.3390/antiox11010128 (2022).
19. Zheng, Y., Zeng, H., She, H., Liu, H. & Sun, N. Expression of peptide NAP in rat retinal Müller cells prevents hypoxia-induced retinal injuries and promotes retinal neurons growth. *Biomed Pharmacother* **64**, 417–423. https://doi.org/10.1016/j.biopha.2010.01.016 (2010).
20. D'Amico, A. G. et al. NAP modulates hyperglycemic-inflammatory event of diabetic retina by counteracting outer blood retinal barrier damage. *J Cell Physiol* **234**, 5230–5240. https://doi.org/10.1002/jcp.27331 (2019).
21. D'Amico, A. G. et al. NAP counteracts hyperglycemia/hypoxia induced retinal pigment epithelial barrier breakdown through modulation of HIFs and VEGF expression. *J Cell Physiol* **233**, 1120–1128. https://doi.org/10.1002/jcp.25971 (2018).
22. D'Amico, A. G. et al. Nap Interferes with Hypoxia-Inducible Factors and VEGF Expression in Retina of Diabetic Rats. *J Mol Neurosci* **61**, 256–266. https://doi.org/10.1007/s12031-016-0869-6 (2017).
23. Beems, E. M. & Van Best, J. A. Light transmission of the cornea in whole human eyes. *Exp Eye Res* **50**, 393–395. https://doi.org/10.1016/0014-4835(90)90140-p (1990).
24. Wang, F. et al. ECM-Like Adhesive Hydrogel for the Regeneration of Large Corneal Stromal Defects. *Adv Healthc Mater* **12**, e2300192. https://doi.org/10.1002/adhm.202300192 (2023).
25. Gouveia, R. M. et al. Assessment of corneal substrate biomechanics and its effect on epithelial stem cell maintenance and differentiation. *Nat Commun* **10**, 1496. https://doi.org/10.1038/s41467-019-09331-6 (2019).
26. Sidney, L. E., McIntosh, O. D. & Hopkinson, A. Phenotypic Change and Induction of Cytokeratin Expression During In Vitro Culture of Corneal Stromal Cells. *Invest Ophthalmol Vis Sci* **56**, 7225–7235. https://doi.org/10.1167/iovs.15-17810 (2015).
27. Uematsu, M. et al. Less Invasive Corneal Transepithelial Electrical Resistance Measurement Method. *Ocul Surf* **14**, 37–42. https://doi.org/10.1016/j.jtos.2015.07.004 (2016).
28. Wilson, S. E. et al. Epithelial injury induces keratocyte apoptosis: hypothesized role for the interleukin-1 system in the modulation of corneal tissue organization and wound healing. *Exp Eye Res* **62**, 325–327. https://doi.org/10.1006/exer.1996.0038 (1996).
29. Golebiowska, A. A., Intravaia, J. T., Sathe, V. M., Kumbar, S. G. & Nukavarapu, S. P. Decellularized extracellular matrix biomaterials for regenerative therapies: Advances, challenges and clinical prospects. *Bioact Mater* **32**, 98–123. https://doi.org/10.1016/j.bioactmat.2023.09.017 (2024).
30. Bordbar-Khiabani, A. & Gasik, M. Smart Hydrogels for Advanced Drug Delivery Systems. *Int J Mol Sci* **23**, https://doi.org/10.3390/ijms23073665 (2022).

31. Wu, K. Y., Qian, S. Y., Faucher, A. & Tran, S. D. Advancements in Hydrogels for Corneal Healing and Tissue Engineering. *Gels* **10**, https://doi.org/10.3390/gels10100662 (2024).
32. Shi, L., Yu, X., Yang, H. & Wu, X. Advanced glycation end products induce human corneal epithelial cells apoptosis through generation of reactive oxygen species and activation of JNK and p38 MAPK pathways. *PLoS ONE* **8**, e66781. https://doi.org/10.1371/journal.pone.0066781 (2013).
33. Huang, C., Liao, R., Wang, F. & Tang, S. Characteristics of Reconstituted Tight Junctions After Corneal Epithelial Wounds and Ultrastructure Alterations of Corneas in Type 2 Diabetic Rats. *Curr Eye Res* **41**, 783–790. https://doi.org/10.3109/02713683.2015.1039653 (2016).
34. Kahn, C. R., Young, E., Lee, I. H. & Rhim, J. S. Human corneal epithelial primary cultures and cell lines with extended life span: in vitro model for ocular studies. *Invest Ophthalmol Vis Sci* **34**, 3429–3441 (1993).
35. Kaluzhny, Y. et al. New Human Organotypic Corneal Tissue Model for Ophthalmic Drug Delivery Studies. *Invest Ophthalmol Vis Sci* **59**, 2880–2898. https://doi.org/10.1167/iovs.18-23944 (2018).
36. Maugeri, G. et al. Protective effect of PACAP against ultraviolet B radiation-induced human corneal endothelial cell injury. *Neuropeptides* **79**, 101978. https://doi.org/10.1016/j.npep.2019.101978 (2020).
37. Bucolo, C. et al. Corneal wound healing and nerve regeneration by novel ophthalmic formulations based on cross-linked sodium hyaluronate, taurine, vitamin B6, and vitamin B12. *Front Pharmacol* **14**, 1109291. https://doi.org/10.3389/fphar.2023.1109291 (2023).
38. Maugeri, G. et al. Modeling diabetic epitheliopathy using 3D-Organotypic corneal epithelium. *Transl Res* **280**, 55–63. https://doi.org/10.1016/j.trsl.2025.05.003 (2025).
39. Alfuraih, S. et al. Effect of High Glucose on Ocular Surface Epithelial Cell Barrier and Tight Junction Proteins. *Invest Ophthalmol Vis Sci* **61**, 3. https://doi.org/10.1167/iovs.61.11.3 (2020).
40. Maugeri, G. et al. Protective effect of pituitary adenylate cyclase activating polypeptide in diabetic keratopathy. *Peptides* **170**, 171107. https://doi.org/10.1016/j.peptides.2023.171107 (2023).
41. Maugeri, G. et al. Nicotine promotes blood retinal barrier damage in a model of human diabetic macular edema. *Toxicol In Vitro* **44**, 182–189. https://doi.org/10.1016/j.tiv.2017.07.003 (2017).
42. D'Amico, A. G. et al. NAP reduces murine microvascular endothelial cells proliferation induced by hyperglycemia. *J Mol Neurosci* **54**, 405–413. https://doi.org/10.1007/s12031-014-0335-2 (2014).

Acknowledgements
The work was carried out as part of the PRIN PNRR 2022, project entitled "SMART peptides-loaded HYdrogel deriVed from acellular cornea: an Innovative Strategy for corneal regeneratION - (Acronym: SmarthyVision)" announcement D.D. n. n. 1409, 14 of February 2022, financed by the European Union – NextGenerationEU".

Author contributions
Material preparation, data collection and analysis were performed by F.B., S.C., A.G.D., N.P., V.D., G.M., E.P., S.S.; conceptualization: F.B., G.M.; Writing – review & editing: F.B., S.C., A.V., G.M.; methodology, formal analysis and investigation, S.C., A.G.D., N.P., V.D., M.P., E.P., G.M.; resources: F.B., D.S., A.L.; samples acquisition: D.S., A.L.; funding acquisition: G.M.; all co-authors reviewed the manuscript. All authors have read and agreed to the published version of the manuscript.

Funding
This research was funded by Italian Ministry of Education, University and Research (MUR) PRIN PNRR 2022, grant number P2022JRBMB, SmarthyVision.

Declarations

Competing interests
The authors declare no competing interests.

Ethical approval
Ethical approval was granted on 19 February 2024; number 09/2024/PAR by the Institutional Review Board of the University of Catania. All data generated or analyzed during this study are included in this published article [and its supplementary information files].

Additional information
Supplementary Information The online version contains supplementary material available at https://doi.org/10.1038/s41598-026-36316-5.

Correspondence and requests for materials should be addressed to G.M.